Int J Solids Structures Vol 18, No 3, pp 205–215, 1982
Printed in Great Britain

0020-7683/82/030205-11$03.00/0
Pergamon Press Ltd

AN INVESTIGATION OF THE STRAIN PATH DEPENDENCE OF THE FORMING LIMIT CURVE

CHIN-CHAN CHU

Scientific Research Laboratory, Ford Motor Company, Dearborn, MI 48121, U S A

(*Received* 26 *November*; *in revised form* 3 *March* 1981)

Abstract—The dependence of the forming limit curve on the deformation history is examined by considering two specific examples of sheet metal forming, representative of two classes of non-proportional strain path: one example is an axisymmetric punch stretching problem, which gives rise to a gradual variation in the strain path from a proportional path; the other example consists of a sheet with residual strains subjected to a proportional stretching so that the complete deformation history, if represented in the principal in-plane strain coordinates, takes a sharp turn. Results are presented for these examples for each of three plasticity theories: flow theory, J_2-deformation theory and the recently proposed corner theory By assuming a plastic potential increment dependent on the direction and magnitude of the incipient plastic strain increment the corner theory gives results which agree qualitatively with experimental observations and therefore seems to be favored for the bifurcation analysis of sheet metal forming problems involving significant strain path variations

1. INTRODUCTION

The concept of using the forming limit curve as a means to characterize the formability of sheet metals has been widely applied for some time. Implied by this idea is the insensitivity of the forming limit curve to the deformation history. However, considering the well-recognized path-dependence of plastic deformation, which is a dominant feature of many sheet metal forming processes, it is expected, and indeed there is experimental evidence [1–4], that the limit states achievable by different forming processes are not the same.

Theoretical studies of formability so far have been mainly focused on proportional stretching, where Hill's bifurcation analysis [5] demonstrated the inadequacy of flow theory in the prediction of localized necking for biaxial stretching. Analytical explanation for the experimentally observed failure by necking in this stretching mode was then sought by Marciniak and Kuczynski via their imperfection model [6], and by Stören and Rice [7], who showed that a constitutive model other than flow theory could display local necking behavior in a sheet of uniform thickness.

Punch stretching, which is of practical interest and, in fact, is commonly used to determine the biaxial stretching quadrant of the forming limit curve, has been analyzed recently [8–10]. Due to the geometric constraints and the existence of an interfacial frictional force between the punch and sheet, the strain distribution is not uniform. As a consequence, the strain path followed by a material element deviates from a proportional strain path. This represents one situation in which the actual forming limit curve can differ from that obtained by assuming proportional straining.

Another type of non-proportional strain path which will be considered is one which features an abrupt alteration, as opposed to the gradual deviation from proportional straining associated with the situation just discussed. Such an abrupt path change would result from a multiple-step forming process like the stretching of a sheet which already contains residual strains.

Stören and Rice's approach will be adopted here. That is, the sheet thickness is assumed uniform prior to the onset of localized necking, which is modelled by a singularity in the incremental equilibrium equation. Of particular interest is the corner theory of plasticity, recently proposed by Christoffersen and Hutchinson [11], which coincides with J_2-deformation theory for nearly proportional loading paths and incorporates a smooth transition to elastic unloading for increasingly non-proportional loading paths.

For punch stretching problems, the forming limit curves were obtained in [10] by employing flow theory and J_2-deformation theory. Therefore, calculations are carried out here for corner theory only. The formulation and results, illustrating the effects of gradual deviation from proportional straining, are presented in Section 2.

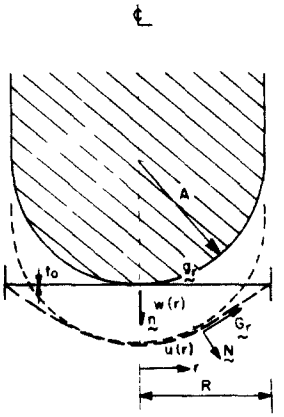

Fig 1. Configuration of a hemispherical punch stretching operation

Proportional stretching after prestraining is studied in Section 3 to reveal the effects of an abrupt strain path change on the forming limit curve.

The results determined by applying the three plasticity theories mentioned are qualitatively compared with experimental results in Section 4 to reveal the degree of suitability of each of these theories in the analysis of sheet metal forming problems.

2. ANALYSIS OF LOCALIZED NECKING FOR PUNCH STRETCHING

2.1 *Formulation*

As shown in Fig. 1, a circular thin sheet of radius R and initial thickness t_0, clamped along its periphery, is stretched over a rigid hemispherical punch of radius A. A Lagrangian formulation, in which a material point is identified by its initial radial distance, r, from the axis of symmetry, is adopted. The incremental virtual work principle within the framework of membrane theory has the form [10]:

$$\int_0^R \left[\dot{\tau}_1\delta\dot{\epsilon}_1 + \dot{\tau}_2\delta\dot{\epsilon}_2 + \tau_1\left(\frac{\mathrm{d}\dot{u}}{\mathrm{d}r}\frac{\mathrm{d}\delta\dot{u}}{\mathrm{d}r} + \frac{\mathrm{d}\dot{w}}{\mathrm{d}r}\frac{\mathrm{d}\delta\dot{w}}{\mathrm{d}r}\right) + \tau_2\frac{\dot{u}}{r}\frac{\delta u}{r}\right] t_0 r\,\mathrm{d}r$$
$$= \int_0^{R^*}\left(\mu p + \frac{p}{A}\dot{u}_t\right)\delta\dot{u}_t r\,\mathrm{d}r \tag{1}$$

where the subscripts 1 and 2 denote the first and second principal directions, which coincide with the radial and circumferential directions respectively and which remain fixed relative to the material throughout the deformation process; $\dot{\epsilon}_\alpha$ are the logarithmic strain increments defined in terms of the horizontal and vertical (as illustrated in Fig. 1) displacement increments $\dot{u}$ and $\dot{w}$ by

$$\dot{\epsilon}_1 = \left[\left(1+\frac{\mathrm{d}u}{\mathrm{d}r}\right)\frac{\mathrm{d}\dot{u}}{\mathrm{d}r} + \frac{\mathrm{d}w}{\mathrm{d}r}\frac{\mathrm{d}\dot{w}}{\mathrm{d}r}\right]\Big/\left[\left(1+\frac{\mathrm{d}u}{\mathrm{d}r}\right)^2 + \left(\frac{\mathrm{d}w}{\mathrm{d}r}\right)^2\right]$$
$$\dot{\epsilon}_2 = \dot{u}/(r+u); \tag{2}$$

and τ_α are the principal Kirchoff stress components related to the corresponding principal Cauchy stress components by

$$\tau_\alpha = J\sigma_\alpha \tag{3}$$

with J being the volume ratio of an element in the deformed configuration to an element in the undeformed configuration.

The r.h.s. of eqn (1) represents the external virtual work done by an increment of the frictional force between the punch and the sheet over the contact area $0 \le r \le R^*$, with R^* increasing as the punch moves downward. Coulomb's law is employed to relate the frictional force to the interfacial pressure, p, which according to membrane theory can be determined by

$$p = (\tau_1 + \tau_2)\, t_0/A. \tag{4}$$

Also appearing on the r.h.s. of eqn (1) is the relative displacement, u_t, of a material point with respect to the rigid translation of the punch. The subscript t is adopted because the relative displacement has a direction tangent to the current sheet surface.

Details of the simplified one-dimensional formulation, eqns (1)–(4), can be found in[10].

2.2 *Constitutive relation*

Of primary interest here is the corner theory recently proposed by Christoffersen and Hutchinson[11]. It is assumed that a corner will be formed at the loading point on the yield surface, and that a plastic potential increment, $\dot{W}^p$, which must satisfy Drucker's postulate, depends on the direction of the continuing loading path at that point. One of the two forms of such a plastic potential increment suggested in[11] and written in terms of the plastic strain increments will be adopted here.

As shown in Fig. 2, ϕ is the angle by which the plastic strain increment deviates from a proportional loading path, whose direction, according to the Mises criterion, coincides with that of the current deviatoric stress tensor in stress space; $\phi = \theta_n$ and $\phi = \theta_0$ represent conical surfaces, the former separating elastic unloading from plastic flow, and the latter bounding the fully active plastic region[12]. The plastic potential increment is assumed to have the form

$$\dot{W}^p = \tfrac{1}{2}\, g\,[\phi\,(\dot{\epsilon}^p{}_{rs})]\, M_{ijkl}\, \dot{\epsilon}^p_{ij}\, \dot{\epsilon}^p_{kl}, \tag{5}$$

where $g(\phi) \equiv 0$ for $\phi \ge \theta_n$ and $g(\phi) \equiv 1$ for $\phi \le \theta_0$. In the transition region, $\theta_0 \le \phi \le \theta_n$, $g(\phi)$ is chosen to be the following function, which gives rise to smoothly varying instantaneous moduli:

$$g(\phi) = (1 - x^m)^{-2} \tag{6}$$

with $x = (\phi - \theta_0)/(\theta_n - \theta_0)$ and $m > 2$. Hereafter the Latin subscripts range from 1 to 3.

Since $g(\phi)$ is identically one in the fully active region, M_{ijkl} in eqn (5) have the meaning of instantaneous plastic moduli for proportional ($\phi = 0$) or near-proportional ($\phi \le \theta_0$) loading. The choice of the instantaneous moduli M_{ijkl} from J_2-deformation theory is thus motivated by the well-known fact that this theory has been more successful than flow theory in bifurcation analyses with the restriction that it is physically unacceptable when dramatic changes occur in

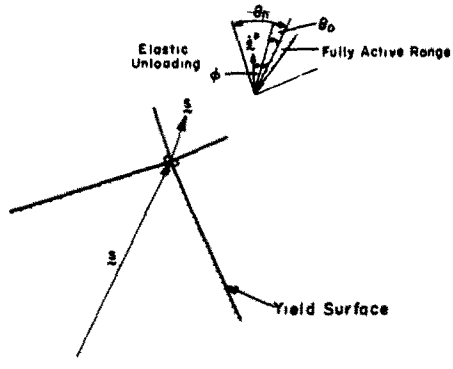

Fig. 2. Schematic representation of the deviation of the plastic strain path from a proportional loading path for a vertex model.

the loading path. Therefore we have

$$M_{ijkl} = \frac{E}{E - E_s}\left\{\tfrac{2}{3} E_s \left[\tfrac{1}{2}(\delta_{ik}\delta_{jl} + \delta_{jk}\delta_{il}) - \tfrac{1}{3}\delta_{ij}\delta_{kl}\right] - \frac{E(E_s - E_t)}{E - E_t}\frac{s_{ij}s_{kl}}{\sigma_e^2}\right\} \tag{7}$$

where E, E_s and E_t are Young's modulus, the secant modulus and the tangent modulus, respectively, as usually defined from a uniaxial true stress-logarithmic strain curve; δ is the Kronecker delta function; σ_e is the flow stress, defined as the larger value of the initial yield stress and the maximum of the effective stress over the stress history; and s_{ij} are the deviatoric stress components. This finite strain version of J_2-deformation theory was first derived by Stören and Rice [7].

By taking the derivative of eqn (5) with respect to ϵ_{ij}^p and inverting the resulting equations, $\dot{s}_{ij} = \partial \dot{W}^p / \partial \dot{\epsilon}_{ij}^p$, we obtain

$$\dot{\epsilon}_{ij}^p = (D\overset{*}{s}_{ij}) + F s_{ij}\dot{\sigma}_e/\sigma_e \tag{8a}$$

or

$$\dot{\epsilon}_{ij}^p = D(\overset{*}{\sigma}_{ij} - \tfrac{1}{3}\delta_{ij}\overset{*}{\sigma}_{kk}) + F(\overset{*}{\sigma}_{kl} - \tfrac{1}{3}\delta_{kl}\overset{*}{\sigma}_{nn})\, s_{ij}s_{kl}/s_{rs}s_{rs} \tag{8b}$$

with

$$D = \tfrac{3}{2}\left(\frac{1}{E_s} - \frac{1}{E}\right)/g(\phi)(1 + l\cot\phi)$$

$$F = \tfrac{3}{2}\left[\left(\frac{1}{E_t} - \frac{1}{E_s}\right) + \frac{l}{(1 + l\cot\phi)\sin\phi\cos\phi}\left(\frac{1}{E_s} - \frac{1}{E}\right)\right]/g(\phi)(1 - l\tan\phi)$$

and

$$l = g'(\phi)/2g(\phi).$$

In eqns (8), (*) denotes the Jaumann derivative of the stress components and is defined as

$$\overset{*}{\sigma}_{kl} = \dot{\sigma}_{kl} + \sigma_{lj}\dot{\epsilon}_{kj} + \sigma_{kj}\dot{\epsilon}_{lj}. \tag{9}$$

The elastic strain increments are given by Hooke's law

$$\dot{\epsilon}_{ij}^e = \frac{1+\nu}{E}\overset{*}{\sigma}_{ij} - \frac{\nu}{E}\delta_{ij}\overset{*}{\sigma}_{kk}. \tag{10}$$

If we assume the total strain increment to be the sum of the elastic and plastic strain increments, then eqns (8) and (10) are combined and inverted to give

$$\overset{*}{\sigma}_{ij} = \hat{L}_{ijkl}\,\dot{\epsilon}_{kl} \tag{11}$$

with

$$\hat{L}_{ijkl} = \frac{1}{\dfrac{1+\nu}{E} + D}\left\{\tfrac{1}{2}(\delta_{ik}\delta_{jl} + \delta_{jk}\delta_{il}) + \frac{E}{1-2\nu}\left(\frac{\nu}{E} + \frac{D}{3}\right)\delta_{ij}\delta_{kl} - \tfrac{3}{2}\frac{F}{\dfrac{1+\nu}{E} + D + F}\frac{s_{ij}s_{kl}}{\sigma_e^2}\right\}$$

where ν in Poisson's ratio.

Equations (11) are written in the present form for the convenience of computation; that is, by replacing D and F with proper values, flow theory and J_2-deformation theory can be

recovered. ($D=0$ and $F=\frac{3}{2}(1/E_t-1/E)$ for flow theory, and $D=\frac{3}{2}(1/E_s-1/E)$ and $F=\frac{3}{2}(1/E_t-1/E_s)$ for J_2-deformation theory.)

For problems with the current principal axes known, as in the present case, we introduce a vector U defined as

$$U_i=1 \quad i=1,\ 2 \text{ and } 3$$

so that (x_iU_i) gives the sum of the components of a vector x and (CU_i) represents a vector with all of its components being equal to C. Equations(11) are then written in a short form in terms of principal components of stress increments and strain increments,

$$\overset{*}{\sigma}_i = L_{ij}\dot{\epsilon}_j$$

with (12)

$$L_{ij}=\frac{1}{\frac{1+\nu}{E}+D}\left\{\delta_{ij}+\frac{E}{1-1\nu}\left(\frac{\nu}{E}+\frac{D}{3}\right)U_iU_j-\frac{3}{2}\frac{F}{\frac{1+\nu}{E}+D+F}\frac{s_is_j}{\sigma_e^2}\right\}.$$

By considering eqns (3) and (9) and neglecting the volume change resulting from elastic deformation, which is small compared to the total deformation, eqns (12) are transformed to

$$\dot{\tau}_i=\hat{C}_{ij}\dot{\epsilon}_j$$

with (13)

$$\hat{C}_{ij}=L_{ij}-2\delta_{ij}\tau_i+\tau_iU_j \text{ (no summation).}$$

The desired incremental stress–strain relations are obtained by employing the plane-stress condition, $\dot{\tau}_3=0$, in eqn (13). Thus, we obtain

$$\dot{\tau}_\alpha=C_{\alpha\beta}\,\dot{\epsilon}_\beta$$

with (14)

$$C_{\alpha\beta}=\hat{C}_{\alpha\beta}-\hat{C}_{\alpha3}\hat{C}_{3\beta}/\hat{C}_{33}.$$

2.3 *Numerical results*

A finite-element method described in[10], which accounts for the moving boundary conditions and the frictional force in the contact region, is employed. The uniaxial stress-strain curve used in the calculations is a modified power law with a continuous tangent modulus at the initial yield point,

$$\frac{\epsilon_e}{\epsilon_y}=\begin{cases}\sigma_e/\sigma_y\\ n(\sigma_e/\sigma_y)^{1/n}-n+1\end{cases} \tag{15}$$

where $\epsilon_e$is the equivalent strain with its increment defined as

$$\dot{\epsilon}_e=\sqrt{(\tfrac{2}{3}\,\dot{\epsilon}_{ij}\,\dot{\epsilon}_{ij})}.$$

Two sets of the parameters m, θ_0, θ_n of $g(\phi)$ are considered: (i) m = 2.5, $\theta_0=0°$, $\theta_n=68°$ and (ii) $m=5.0$, $\theta_0=34°$, $\theta_n=68°$. The first set is chosen because it was shown in [11] to most closely reproduce the ratio of instantaneous effective shear modulus to the elastic shear modulus, obtained from a self-consistent model of a polycrystal [13], as a function of ϕ. The second set is included to demonstrate the influence of these parameters on the results.

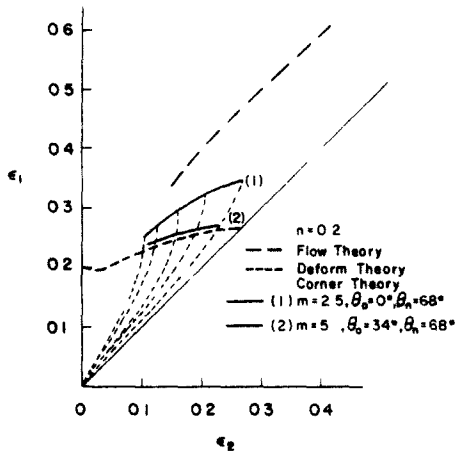

Fig 3 Forming limit curves obtained from punch stretching problems for three constitutive models with strain hardening exponent $n = 0.2$, with each of the dashed curves representing the strain path followed by the critical material point

Since the instantaneous moduli $C_{\alpha\beta}$ of corner theory depend on the yet-to-be-determined plastic strain increment, iteration is necessary for each incremental step. However, to save computing time, the current plastic strain increment is approximated by the increment obtained from the previous step. The error involved can be limited if sufficiently small steps are used.

As in [10], the value of the frictional coefficient, μ, ranging from 0.0 to 0.75, plays the role of varying the uniformity of the strain distribution and hence the strain ratio of the critical strain state.

Unlike flow theory, from which no bifurcation can be predicted for inplane as well as out-of-plane biaxial stretching, but similar to J_2-deformation theory, the corner theory adopted here results in a singular equilibrium equation at a realistic strain level. The maximum strain reached at the onset of such a singularity is used to construct the forming limit curve.

Illustrated in Figs. 3 and 4 are the forming limit curves for cases with the strain hardening exponent $n = 0.2$ and 0.5 respectively. Results for $n = 0.125$ are similar to those in Fig. 3 and therefore are not diaplayed. It is observed from Fig. 3 that, for moderate and low strain hardening materials, the forming limit curve obtained by the corner theory attains a higher major principal strain than that obtained by J_2-deformation theory, but lies at a major principal strain level lower

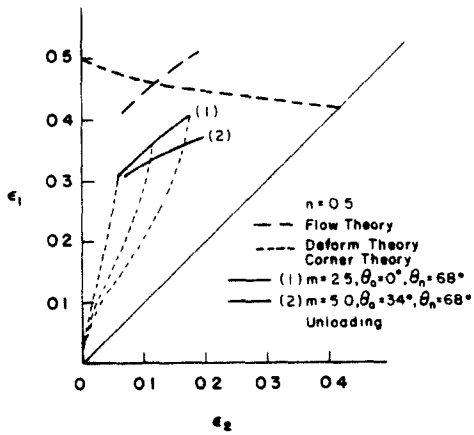

Fig 4. Forming limit curves obtained from punch stretching problems for three constitutive models with strain hardening exponent $n = 0.5$, with each of the dashed curves representing the strain path followed by the critical material point and dotted curve representing the strain state at which unloading first occurs

than that obtained by flow theory. By increasing m and/or θ_0, the resulting limit curve converges to that predicted by J_2-deformation theory.

Figure 4 shows that for high strain hardening materials the forming limit curves obtained lie at lower major principal strain levels than those from J_2-deformation theory as well as those from flow theory. This is because localization of strain is accelerated by elastic unloading in part of the sheet, which, for the present theory, occurs at a strain level approximately the same as that predicted by J_2-deformation theory but, due to less stiffness, much lower than that predicted by flow theory. A higher limit strain by J_2-deformation theory, on the other hand, results from the fact that the same modulus is adopted for both loading and unloading branches, which allows further distribution of the strain increments over a wider area and hence a later development of instability.

Since for in-plane proportional stretching corner theory predicts the same limit curve as J_2-deformation theory does, and the latter gives the same limit curve for punch stretching and in-plane stretching, comparison of the present results with those from J_2-deformation theory also illustrates the differences between the forming limit curves obtained by punch stretching and by in-plane stretching when corner theory is adopted. Figures 3 and 4 therefore indicate that for low and moderate strain hardening materials, the limit strains achievable by punch stretching are higher than those achievable by proportional stretching. However, for high strain hardening materials, the opposite situation results.

3. ANALYSIS OF LOCALIZED NECKING FOR IN-PLANE STRETCHING INVOLVING PATH CHANGES

3.1 *Formulation*

As derived by Stören and Rice in [7], an incipient non-uniform flow field $\mathbf{f}$ across a band, with unit normal $\mathbf{n}$, has to satisfy the incremental equilibrium equations

$$(n_\beta \sigma_{\alpha\beta} M_{\gamma\xi} n_\xi + n_\beta L_{\alpha\beta\gamma\xi} n_\xi) f_\gamma = 0. \tag{16}$$

Here $L_{\alpha\beta\gamma\xi}$ are the instantaneous moduli relating the Cauchy stress increments and the strain increments. They can be obtained from eqns (9) and (11) and the plane-stress condition as

$$L_{\alpha\beta\gamma\xi} = \hat{L}_{\alpha\beta\gamma\xi} - \hat{L}_{\alpha\beta 33} M_{\gamma\xi} - \tfrac{1}{2}(\sigma_{\beta\xi}\delta_{\alpha\gamma} + \sigma_{\alpha\gamma}\delta_{\beta\xi} + \sigma_{\alpha\xi}\delta_{\beta\gamma} + \sigma_{\beta\gamma}\delta_{\alpha\xi}) \tag{17}$$

with $M_{\gamma\xi}$ representing the ratio of the thickness strain increment, $\dot{\epsilon}_{33}$, to the in-plane strain increment $\epsilon_{\gamma\xi}$, or

$$M_{\gamma\xi} = -L_{33\gamma\xi}/L_{3333}. \tag{18}$$

Localized necking is considered possible when a non-zero flow field $\mathbf{f}$ exists; that is, when the determinant of the coefficients in eqns (16) is zero.

3.2 *Solution*

To examine the effect of an abrupt path change on the forming limit curve, a simple two-step stretching process, as described in the following diagram, is considered.

$$\{\sigma_e = \sigma_y, \boldsymbol{\sigma} = \mathbf{0}, \boldsymbol{\epsilon} = \mathbf{0}\}$$
$$\downarrow$$
$$\text{Step (1)}$$
$$\downarrow$$
$$\{\sigma_e = \beta_1 \sigma_1^{(1)}, \boldsymbol{\sigma}^{(1)} = (\sigma_1^{(1)}, \alpha_1 \sigma_1^{(1)}, 0), \boldsymbol{\epsilon}^{(1)} = (\epsilon_1^{(1)}, \rho_1 \epsilon_1^{(1)}, \gamma_1 \epsilon_1^{(1)})\}$$
$$\downarrow$$
$$\text{Unloading}$$
$$\downarrow$$
$$\{\sigma_e = \beta_1 \sigma_1^{(1)}, \boldsymbol{\sigma}^{(0)} = \mathbf{0}, \boldsymbol{\epsilon}^{(0)} = (\epsilon_1^{(0)}, \epsilon_2^{(0)}, \epsilon_3^{(0)})\}$$
$$\downarrow$$
$$\text{Step (2)}$$
$$\downarrow$$
$$\{\sigma_e = \beta_2 \sigma_1^{(2)}, \boldsymbol{\sigma}^{(2)} = (\sigma_1^{(2)}, \alpha_2 \sigma_1^{(2)}, 0), \boldsymbol{\epsilon}^{(2)} = (\epsilon_1^{(0)} + \epsilon_1^{(2)}, \epsilon_2^{(0)} + \rho_2 \epsilon_1^{(2)}, \epsilon_2^{(0)} + \gamma_2 \epsilon_1^{(2)})\}$$

where Steps (1) and (2) are proportional strain paths with strain ratio ρ_1 and ρ_2, respectively. The residual strain $\epsilon^{(0)}$ is the plastic part of $\epsilon^{(1)}$ The constants α,β and γ are functions of the strain ratio and Poisson's ratio. Flow stress σ_e, as defined earlier, is the larger value of the initial yield stress and the maximum of the effective stress over the stress history. Note that while the initial yield stress is σ_y for Step (1), it is raised to $\beta_1\sigma_1^{(1)}$ for Step (2).

Since J_2-deformation theory is not physically acceptable when unloading occurs, only flow theory and corner theory will be considered here.

Before carrying out the incremental calculations, which include solving for the stress and strain fields and checking the uniqueness of these solutions, eqns (16), the problem can be better addressed if the approximation of neglecting the elastic deformation is adopted. As a result of this approximation, α, β and γ are related to ρ by

$$\alpha = (1+2\rho)/(2+\rho), \beta = \sqrt{(3(1+\rho+\rho^2))}/(2+\rho) \text{ and } \gamma = -(1+\rho). \tag{19}$$

Since the current stress field, $\boldsymbol{\sigma}$, and the instantaneous modulus, **L**, during the second stretching process are determined by the strain increment $\dot{\epsilon}_i$, the onset of an instability of the strain field is thus unaffected by the residual strain $\epsilon^{(0)}$. Therefore, eqns (16) require attainment of the same stress state to trigger localized necking as required in a one-step proportional stretching problem with strain ratio ρ_2. Consequently the equivalent strain at this limit stress state may be determined from the corresponding one-step proportional stretching problem, as in [5, 7]. Alternatively it may be obtained by integrating the strain increment through the two-step stretching process being examined here. The necessary equivalence of these two expressions gives

$$\sqrt{(\tfrac{2}{3}(1+\rho_1+\rho_1^2))}\,\epsilon_1^{(0)} + \sqrt{(\tfrac{2}{3}(1+\rho_2+\rho_2^2))}\,\epsilon_1^{(2)} = \sqrt{(\tfrac{2}{3}(1+\rho_2+\rho_2^2))}\,\epsilon_1^*, \tag{20}$$

which can be rearranged to give the limit value for the major principal strain in the two-step process as

$$(\epsilon_1)_{\lim} = \epsilon_1^* + (1 - \sqrt{((1+\rho_1+\rho_1^2)/(1+\rho_2+\rho_2^2))})\,\epsilon_1^{(0)} \tag{21}$$

where ϵ_1^* is the limit major principal strain obtained from the corresponding proportional stretching problem.

Equation (21) can be used to construct the forming limit curve for various values of ρ_1, ρ_2 and $\epsilon_1^{(0)}$. It also clearly demonstrates that

$$(\epsilon_1)_{\lim} \gtrless \epsilon_1^* \text{ when } \rho_2 \gtrless \rho_1 \tag{22}$$

The value of ϵ_1^* predicted by flow theory for biaxial stretching is known to be unreasonably high; eqn (21) thus gives only part of the forming limit curve , as shown in Fig. 5 where cases with $\rho_1 = 1.0$ and -0.5 with several $\epsilon_1^{(0)}$ values are plotted for materials with $n = 0.2$. It can be observed that some strain states with negative strain ratios, which are unreachable by a single-step proportional stretching, are predicted to be free of localization phenomena if a uniaxial prestrain is imposed. On the other hand, localized necking, which is excluded for all biaxial stretching, can occur at certain biaxial strain states if the sheet is prestretched biaxially.

If corner theory is employed, ϵ_1^* obtained by Stören and Rice[7], is used in eqn (21). The resulting forming limit curves for $n = 0.2$ and 0.4 are displayed (as dashed curves) in Figs. 6 and 7 respectively. These figures show that V-shaped forming limit curves are obtained for the $\rho_1 = 1.0$ and $\rho_1 = -0.5$ cases, even for high strain hardening materials for which a flattened or even falling biaxial branch of the limit curve is predicted for proportional stretching. The minimum point of such a V-shaped curve, compared with Stören and Rice's result, is seen to be lower for sheets with biaxial prestrain and higher for sheets with uniaxial prestrain.

As mentioned earlier, the elastic strain has been neglected in the above approximation. Numerical calculations carried out incrementally show that while the elastic part of the deformation has negligible influence on the previous results if flow theory is employed, it can result in a significant difference in the corner theory solution, the magnitude of this difference

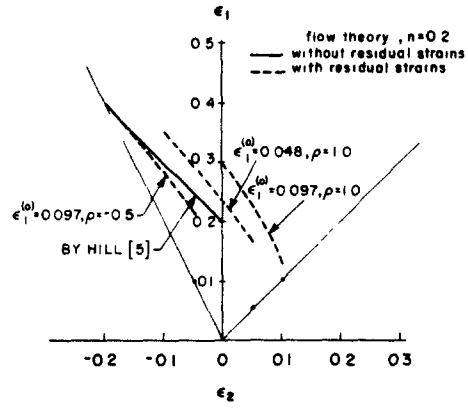

Fig. 5 Effect of biaxial and uniaxial prestretching, predicted by flow theory with strain hardening exponent $n = 0.2$, on the forming limit curves for in-plane stretching processes.

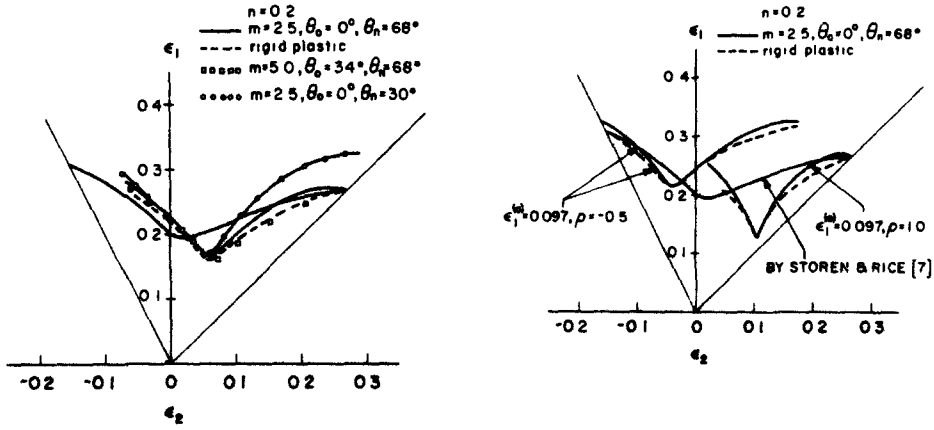

Fig. 6. Effect of biaxial and uniaxial prestretching, predicted by corner theory with strain hardening exponent $n = 0.2$, on the forming limit curves for in-plane stretching processes. (a) $\epsilon_1^{(0)} = 0.048$, $\rho_1 = 1.0$; (b) $\epsilon_1^{(0)} = 0.097$, $\rho_1 = -0\,5$ and $1\,0$

depending mainly on how the parameters m, θ_0 and θ_n are chosen. Figures 6 and 7 show the results of these numerical calculations for corner theory including the elastic deformation, employing the same two sets of parameters for $g(\phi)$ as in Section 2.3; the data obtained from the first set are displayed as solid lines. They differ most greatly from the approximated results at both ends of the curves. By increasing m and/or θ_0, the difference diminishes as illustrated by the square symbols in Figs. 6(a) and 7(a). As a check of the results, a yield surface with a more blunted corner ($m = 2.5$, $\theta_0 = 0$, $\theta_n = 30°$) is also considered. In this case, even a minor deviation of the plastic strain increment from the proportional path can stimulate a much stiffer material reaction, which therefore leads to a prediction closer to that of flow theory, as illustrated by circles in Figs. 6(a) and 7(a).

Finally it should be pointed out that in the calculation the material is assumed to yield during the second stretching process only after the previous maximum equivalent stress level is attained. This is of course an approximation which ignores the anisotropy that vertex formation necessitates. Therefore, further investigations which take into account this developing anisotropy of the yield surface are desirable.

4 DISCUSSION

For the problems considered in the previous Sections, a few experimental results are available for qualitative comparison. In [1,2], it was observed that the forming limit curves obtained by punch stretching attain higher values of the limiting major principal strain than

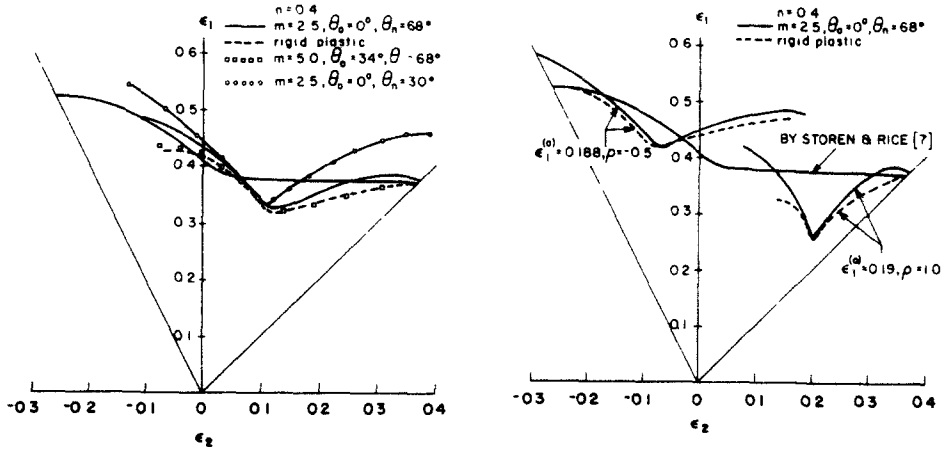

Fig. 7 Effect of biaxial and uniaxial prestretching, predicted by corner theory with strain hardening exponent $n = 0.4$, on the forming limit curves for in-plane stretching processes (a) $\epsilon_1^{(0)} = 0.092$, $\rho_1 = 1.0$; (b) $\epsilon_1^{(0)} = 0.19$, $\rho_1 = -0.5$ and 1.0

those obtained by in-plane stretching. As shown in [10], flow theory predicts the opposite trend; that is, for the axisymmetric punch stretching problem, localization of strain can be initiated at a strain level much lower than that for proportional loading. Neither are J_2-deformation theory's results—a unique forming limit curve independent of the deformation history—compatible with experimental observations. The presently adopted corner theory, however, by assuming a higher instantaneous modulus for an increasingly non-proportional strain path, does result in higher formability for the punch stretching process than for the in-plane stretching process for low and moderate strain hardening materials. For high strain hardening materials the disagreement between the analytical and experimental results, which is greatest for a nearly plane-strain stretching mode in which the strain distribution is highly non-uniform, can be attributed to the early occurrence of unloading in part of the sheet during a punch stretching process. The disagreement is expected to be minimized if the material's rate sensitivity is taken into account.

In [3,4], experiments demonstrated that the limit major principal strain is raised and lowered due to the existence of biaxial and uniaxial prestrains respectively. These effects of the prestrain are qualitatively predicted by corner theory, as shown in Section 3. However, the phenomenological corner theory is not necessarily the only way to explain the influence from prestretching. In fact, according to eqn (21), the same effect can also be obtained by flow theory except that in this case the predicted value of $\epsilon_1^\dagger$ for biaxial stretching is too high to be realistic. Therefore, Marciniak and Kuczynski's [6] model, for example, with its assumed intial imperfection to instigate necking for biaxial stretching mode, should also be able to predict qualitatively the effects of the prestrain on the forming limit curve.

It is interesting to notice that eqn (21) was proposed in [4], although without justification. The analysis in this paper, on the other hand, is based on the assumption that no residual stresses are present after unloading, and this is generally not true.

Further studies involving more complicated path changes are desirable in order to have a complete view of the path dependence of the forming limit curve. But the present study demonstrates that the corner theory of plasticity proposed in [11] is favored for the bifurcation analysis of sheet metals subjected to forming processes with dramatic path changes.

Acknowledgement—The author wishes to thank S. C. Tang and S. K. Samanta for their helpful comments and review of this paper.

The support of this work by the Scientific Research Laboratory at Ford Motor Company is appreciated.

REFERENCES

1. A. K. Ghosh and S. S. Hecker, Stretching limits in sheet metals: in-plane versus out-of-plane deformation. *Met. Trans* **5**, 2161 (1974).
2. S. Hecker, Sheet stretching experiments *Application of Numerical Methods to Forming Processes*, **85**, ASME (1978)

3. J. Laukonis and A. K. Ghosh, Effects of strain path changes on the formability of sheet metals. *Met. Trans. A* **9A**, 1849 (1978).
4. H. J. Kleemola and M. T. Pelkkikangas, Effect of predeformation and strain path on the forming limits of steel, copper and brass. *Sheet Metal Indust.* 591 (1977).
5. R. Hill, On discontinuous plastic states, with special reference to localized necking in thin sheets. *J. Mech. Phys. Solids* **1**, 19 (1952).
6. A. Marciniak and K. Kuczynski, Limit strains in the process of stretch forming sheet metal. *Int. J. Mech. Sci.* **9**, 609 (1967).
7. S. Stören and J. R. Rice, Localized necking in thin sheets. *J. Mech. Phys. Solids* **23**, 421 (1975).
8. B. Kaftanoglu and J. M. Alexander, On quasistatic axisymmetrical stretch forming. *Int. J. Mech. Sci.* **12**, 1065 (1970).
9. N. M. Wang and B. Budiansky, Analysis of sheet metal stamping by a finite element method. *J. Appl. Mech.* **45**, 73 (1978).
10. C. C. Chu, An analysis of localized necking in punch stretching. *Int. J. Solids Structures* **16**, 913 (1980).
11. J. Christoffersen and J W. Hutchinson, A class of phenomenological corner theories of plasticity *J. Mech. Phys. Solids* **27**, 465 (1979).
12 R. Hill, The essential structure of constitutive laws for metal composites and polycrystals. *J. Mech. Phys. Solids* **15**, 79 (1967).
13. J. W. Hutchinson, Elastic-plastic behavior of polycrystalline metals and composites. *Proc. Roy. Soc. London* A **319**, 247 (1970).